Hindawi Publishing Corporation
Advances in OptoElectronics
Volume 2016, Article ID 5843636, 7 pages
http://dx.doi.org/10.1155/2016/5843636

Research Article

Noise Gain Features of Fiber Raman Amplifier

Georgii S. Felinskyi and Mykhailo Y. Dyriv

Taras Shevchenko National University of Kyiv, 4g, Academician Glushkov Prospect, Kyiv 03022, Ukraine

Correspondence should be addressed to Georgii S. Felinskyi; felinskyi@yahoo.com

Received 21 April 2016; Accepted 14 June 2016

Academic Editor: Somenath N. Sarkar

The formation dynamics of the optical noise in a silica single mode fiber (SMF) as function of the pump power variation in the counter pumped fiber Raman amplifier (FRA) is experimentally studied. The ratio between the power of amplified spontaneous emission and the power of incoherent optical noise is quantitatively determined by detailed analysis of experimental data in the pump powers range of 100–300 mW within the full band of Stokes frequencies, including FRA working wavelengths over the C + L transparency windows. It is found out the maximum of Raman gain coefficient for optical noise does not exceed ~60% of corresponding peak at the gain profile maximum of coherent signal. It is shown that the real FRA noise figure may be considerably less than 3 dB over a wide wavelength range (100 nm) at a pump power of several hundreds of mW.

1. Introduction

The fiber optic amplifiers based on the effect of stimulated Raman scattering were the first practical devices of nonlinear optics widely used in the high-speed and long distance telecommunication [1, 2].

It is commonly accepted in digital communication systems to use the bit error rate (BER) B_{er} as a generalized quality parameter to describe the statistical probability of the bit errors occurrence [3]. In the fiber line it is clearly expressed by the optical signal to noise ratio (OSNR) $Q = P_s/P_n$, where P_s and P_n are the optical powers of signal and noise waves, respectively. The OSNR should be changed at the simultaneous gain of the signal and noise optical waves from Q_{in} at FRA input to Q_{out} at amplifier output. B_{er} of the standard configuration consisting of the optical link and the FRA is a function of Q_{out} [4] and reads as follows:

$$B_{er} = \frac{1}{2}\mathrm{Erfc}\left(\sqrt{\frac{Q_{out}}{8}}\right), \quad \text{here } Q_{out} = \frac{Q_{in}}{N_f}, \tag{1}$$

where $\mathrm{Erfc}(x)$ is the complementary error function and N_f is noise figure of FRA. N_f can significantly change B_{er}. For example, if $Q_{out} = 21.6$ dB then $B_{er} = 10^{-9}$ and the +1 dB or −1 dB at this OSNR level leads to reduction or increasing B_{er} by one order of its value.

The phenomenological noise theory [5–7] establishes the lower "quantum limit" of N_f at the level of 3 dB in any optical amplifiers. However, the almost complete absence of FRA effect on the B_{er} degradation is observed [8] just at the start of FRA application. It is shown in the early 2000s [3, 4, 9] that one can really achieve $B_{er} \sim 10^{-12}$ without any additional methods for error correction in the terabit telecommunication over the distance of many hundred kilometers. Therefore the analysis of reasons for the apparent mismatch between actual noise theory and its application has great practical interest. The additional experimental studies are also required to clarify the FRA noise gain features.

In general, the linear approach to electronic equivalent circuits used in the phenomenological theory is unacceptable to the description of such nonlinear processes as Raman light scattering. Unfortunately this conventional theory results in too much overstated estimations of the FRA own noise because of photon-phonon interaction and nonlinear nature of the stimulated light scattering that are not taken into account. So, we will consider two fundamental reasons of FRA low noise. Firstly, it is the optical noise formation due to spontaneous Raman scattering. Secondly, the stimulated light

scattering results to the nonlinear amplification of noise and signal waves exponentially increased with pumping power P_p.

2. Fundamentals of the Spontaneous and Stimulated Light Scattering

The common basis for both signal fiber gain and optical noise amplification is the fundamental physical processes of elastic and inelastic light scattering. Coherent signal wave is effectively amplified in a single mode fiber by stimulated Raman scattering using the relatively small pump power. Backward part of elastic Rayleigh scattering can lead to the signal distortion due to strong interference of delayed signal wave reflections. The main source of amplifier optical noise is initially formed by spontaneous Raman scattering (SRS) from the pump.

Rayleigh scattering cross section σ_r and SRS cross section σ_T do not depend on their excitation wave intensities. Thus both these effects are referred to as linear optical effects [1, 3, 9]. The absolute value is $\sigma_r \sim 10^{-3}$ in comparison to the excitation wave intensity and the corresponding value for SRS is $\sigma_T \sim 10^{-6}$.

Rayleigh scattering is elastic; therefore it resulted in coherent wave with $\omega_r = \omega_p$, where ω_r and ω_p are frequencies of the scattered wave and the pumping wave, respectively. Scattered wave in the Stokes Raman scheme is inelastic and it appears with shifted frequency $\omega_s = \omega_p - \omega_v$, where ω_v is the phonon frequency, that is, the own vibration frequency of molecules in the fiber core.

Stokes wave at SRS process is not coherent since it is formed involving the thermal phonons with arbitrary phase of vibration frequency ω_v. Thus spontaneous Stokes waves are obtained with random phase distribution at the frequency ω_s. Therefore, the intensity of Stokes spectrum components at SRS process is directly proportional to phonon population factor (n_B+1); here $n_B = n_B(\omega_v, T) = [\exp(\hbar\omega_v/kT)-1]^{-1}$ that is depended on vibration frequency ω_v and temperature T.

The stimulated Raman amplification occurred at the same Stokes frequency $\omega_s = \omega_p - \omega_v$ as SRS. It is independent of the phonon population density. Therefore it is independent of the temperature. Practically, this means that only nonequilibrium phonons affect the stimulated Raman gain. One can assume that $n_B = 0$ that leads to $T = 0$. As a result, the spectral response of stimulated amplification, that is, the Raman gain profile $g_R \sim \sigma_0$, repeats the SRS spectrum at $T = 0$ [1]:

$$\sigma_0(\omega_v) = \frac{\sigma_T(\omega_v)}{n_B(\omega_v, T) + 1}, \tag{2}$$

where σ_0 is well known as zero Kelvin cross section.

The spontaneous Raman cross section and Raman gain profile for standard silica fiber are shown in Figure 1. The essential difference between spontaneous Raman spectrum and Raman gain profile according to (2) and the data on Figure 1 should be observed in the frequency region of Stokes shift less than 6 THz = 200 cm^{-1}. In more high-frequency area the thermal density factor of Stokes phonon numbers (>400 cm^{-1}) loses its frequency dependence, practically not

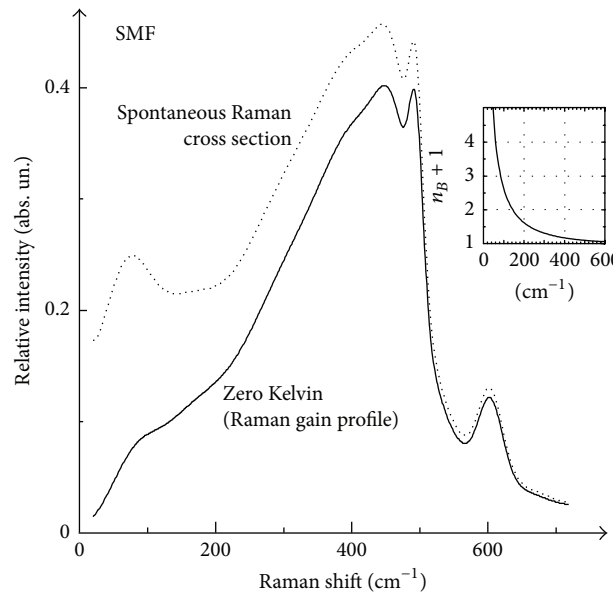

Figure 1: Spontaneous Raman spectrum (dotted line) and Raman gain profile (solid line) in Stokes shifted frequency area from 0 to 21 THz (700 cm^{-1}) for standard silica fiber. Thermal phonon factor as function of Raman shift frequency at $T = 300$ K is shown on the right hand inset.

differing from unit. Consequently, the spontaneous Raman spectrum coincides with the Raman gain profile.

The Raman gain profile $g_R(\omega_v)$ may be expressed by the zero Kelvin cross section $\sigma_0(\omega_v)$ as [10]

$$g_R(\omega_v) = \sigma_0(\omega_v) \cdot \frac{\lambda_s^3}{c^2 h A_{\text{eff}}^{ps} n_p^2} \tag{3}$$

or by the third-order susceptibility tensor components $\chi_{ijkl}^{(3)}$ as [11]

$$g_R = -\frac{3\omega_s}{\varepsilon_0 c^2 n_p n_s} \frac{\text{Im}\left[\chi_{iiii}^{(3)} + \chi_{ijji}^{(3)}\right]}{2A_{\text{eff}}^{ps}}, \tag{4}$$

where A_{eff}^{ps} is the effective area of the pump and signal overlapping region, λ_s is the Stokes wavelength, n_p and n_s are the refractive indexes of fiber core at pump and Stokes wavelengths, respectively, c is the speed of light, h is Plank's constant, and ε_0 is the dielectric constant.

The dynamics of Raman amplification is defined by the Raman gain profile $g_R(\omega)$. Stokes power $P_s(z, \omega)$ variation by power $P_p(z)$ of the monochromatic pumping wave in arbitrary fiber coordinate z is described by the coupled equations [12]:

$$\begin{aligned} \frac{dP_s(z,\omega)}{dz} &= g_R(\omega) P_p(z) P_s(z,\omega) - \alpha_s P_s(z,\omega), \\ \frac{dP_p(z)}{dz} &= -\frac{\omega_p}{\omega_s} g_R(\omega) P_p(z) P_s(z,\omega) - \alpha_p P_p(z), \end{aligned} \tag{5}$$

where α_s and α_p are the dumping constants for the Stokes and pump waves, respectively. The analytical solution of equations

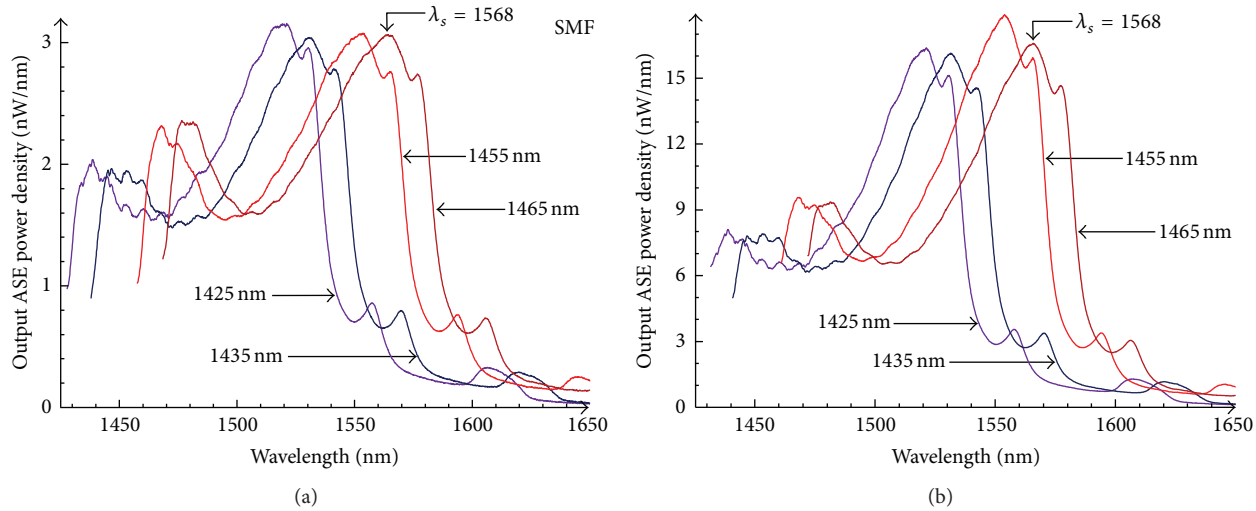

FIGURE 2: Spontaneous emission spectra of the counter pumped SMF fiber by input power of 100 mW (a) and 300 mW (b) at coherent signal absence.

of system (5) may be written in the special case using the approximation of no pump depletion:

$$P_s(L) = P_s(0)\exp\left(g_R P_0 L_{\text{eff}} - \alpha_s L\right), \quad (6)$$

where $L_{\text{eff}} = [1 - \exp(-\alpha_p L)]/\alpha_p$ is effective length; P_0 is initial pump power, and $P_0 = P_p(L)$ in the case of backward pumping.

Note the value of g_R in (4) is the gain coefficient for coherent signal with the power recharged by the power of coherent pumping wave.

The random phase distribution of noise Stokes waves for each fixed frequency ω_s is a reason of a significant phase mismatch between the noise and the pump waves. Taking this fact into account we assume that the Raman gain coefficient g_N for Stokes noise can be significantly less than g_R; that is,

$$g_N = \eta g_R, \quad 0 < \eta < 1. \quad (7)$$

We present the results of our experimental studies of Stokes noise gain in single mode fiber. It allows us to quantify the introduced gain coefficient g_N for the Stokes noise and the η parameter.

3. Study of Stokes Noise Amplification in Single Mode Fiber

Amplified spontaneous emission (ASE) spectra from the 50 km span of standard single mode fiber (SMF) were observed by us using the FRA unit with four laser diodes (LD) as pump sources. These spectra are measured with spectral resolution of 1 nm (~4 cm^{-1}) in opposite direction to the pump waves with respective wavelengths 1425, 1435, 1455, and 1465 nm. The experimental setup was previously described in [1].

3.1. Analysis of the Spontaneous and Stimulated Emission Spectra at the Counter Pumping. Spontaneous emission spectra were studied on idle amplifier, that is, in the signal absence. The spectra recording was carried with a resolution of 1 nm. So we observed very intense Rayleigh scattering lines from each pumping LD. Its power was 10^3 times higher than the integrated power of the full Stokes spectrum.

Each spectrum of Stokes radiation as shown in Figure 2 is shifted by wavelength according to the pump wavelength. Powerful lines of Rayleigh scattering are removed from the image. Absolute values of power on the vertical axis are shown for the 100 mW pump power (Figure 2(a)) and for the 300 mW pump power (Figure 2(b)).

At least two major features are presented in all spectra shown in Figure 2(a). First, the integrated power of Stokes continuum does not exceed ~10^{-3} from the total power of Rayleigh scattering lines. This ratio is typical for pure spontaneous Raman scattering as its cross section is independent on the excitation power. Second, strongly pronounced local maxima in all spectra in Figure 2(a) are indicated to the spontaneous character of output Raman power at P_p = 100 mW. These maxima are localized within the wavelength range corresponding to the Stokes shifts up to 200 cm^{-1} clearly (see Figure 1). In addition, the stimulated Raman scattering is a threshold effect. It may appear only above a certain critical pumping power. Pumping power thresholds for the Stokes wave amplification in certain fibers were determined by us earlier in [13]. In particular, the Raman gain threshold is equal to $P_p^{\text{th}} \approx 120$ mW for the studied fiber at the wavelength of 1550 nm [13]. *S*, incoherent Stokes noise, can be generated during the whole fiber length at the pumping with input power no more than 100 mW.

However if the pump power is increased by threefold (from 100 mW to 300 mW) then the output ASE power is increased more by 5 times (Figure 2(b)). The peak intensities

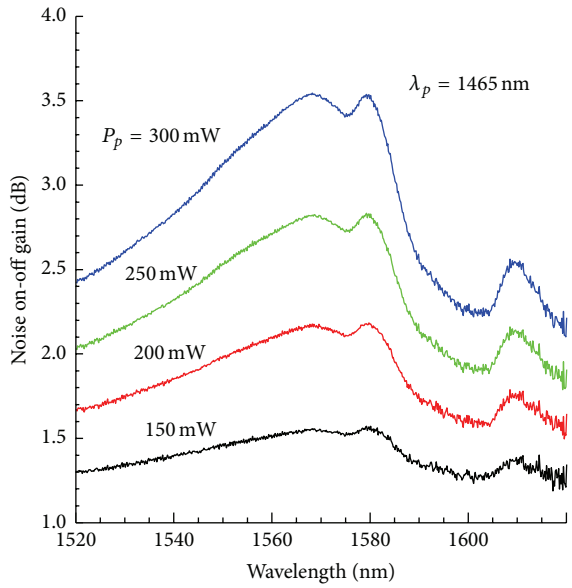

FIGURE 3: «On/Off» Raman gain spectra of the internal optical noise in single mode silica fiber at several pumping powers. Spontaneous Raman scattering intensity corresponded to 0 dB level.

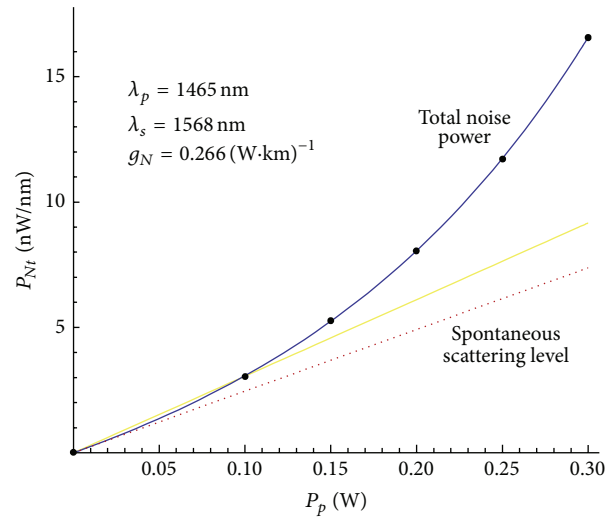

FIGURE 4: Nonlinear fitting results (solid line) of our experimental data (black circles) with a model function (8). Output noise power level when the Raman gain is "turned off" is shown by dotted direct line.

in the smaller wavelength area of ASE spectra are decreased relative to the main power peak (gain maxima). It definitely indicates the essentially nonlinear nature of optical noise amplification at pumping power of 300 mW. So ASE is a main part of total optical noise of amplifier as a mixture of spontaneous and stimulated Raman scattering. Further we will consider the formation dynamics of the Raman gain by the pump power.

3.2. Raman Gain Dynamics and Pump Power. We have analyzed the output ASE power spectra in Stokes range 20–700 cm^{-1}. It is as a function of input pump power for all four pump wavelengths used in our experiment.

We used the Stokes continuum at $P_p = 100$ mW to scale the optical noise spectra by the pumping power changing in amplifier. The spectral distribution of ASE output is more than 90% of the profile of the spontaneous Raman scattering (SRS). This means that all SRS spectral components have the linear variation due to pump power. The SRS may be considered as the optical noise level at a Raman gain. It is conventionally set to "Off."

As a result, the ratio $G_{\text{on-off}} = P_{Nt}/P_{Ns}$, where P_{Nt} is the total power of optical noise as a sum of stimulated and spontaneous terms and P_{Ns} is the pure spontaneous noise power, can be considered as an «On/Off» gain of optical noise. «On/Off» ASE spectra for the upper threshold gain powers at $\lambda_p = 1465$ nm for the typical range of amplifier working wavelengths are shown in Figure 3. As one can see in Figure 3, the gain spectrum reached its highest value within the total C + L telecommunication windows. It is equal to 3.5 dB at the wavelength of 1568 nm with $P_p = 300$ mW.

We registered the maximum possible ASE power under the terms of our experiment in the whole working wavelengths band (see Figure 2). The shapes of the «On/Off» ASE gain spectra and its maxima for other pumping wavelengths used in our experiment are quite similar to those described in Figure 3 for $\lambda_p = 1465$ nm. So the presented estimation for the «On/Off» ASE gain $G_{\text{on-off}} = 3.5$ dB at $P_p \leq 300$ mW can be regarded to an upper limit for single mode silica fiber in the wavelength range of 1520–1620 nm.

Thus, the gain of optical noise is more than twice higher than the SRS power in the pure silica fiber even at the maximum pump power. Since the SRS cross section is $\sigma_T \sim 10^{-6}$ then pump energy costs for the noise gain can be neglected in the entire pumping power range. So the analytical expression (6) based on no pump depletion approximation can be applied for quantitative evaluation of ASE Raman gain coefficient and its spectral profile. It was confirmed by our numerical solution of (5) using the Runge-Kutta fourth-order method.

Also it is found that the Raman gain of coherent signal ($g_{R\max} = 0.38$ W^{-1}·km^{-1} [12]) is $G_{\text{on-off}} = 8.3$ dB at $P_p = 300$ mW. This value substantially exceeded the noise «On/Off» gain. That fact directly points on the difference between the noise gain coefficient g_N and the gain coefficient g_R for coherent signal.

The growth dynamics of particular noise spectral component is shown in Figure 4 for selected spectral component at wavelength of 1568 nm. It is located at the maximum of Stokes noise spectrum from pumping of $\lambda_p = 1465$ nm (see Figure 2). The straight line of spontaneous scattering level as discussed in Section 1 is a result of steady Raman cross section regardless of specific fiber type.

The curve nonlinearity for "total noise power" in Figure 4 is caused by the effect of stimulated Raman scattering. Both curves in Figure 4 are different at $P_p \leq P_p^{\text{th}}$ due to the almost

complete absence of stimulated Raman scattering. Really total power output of the amplifier optical noise at $P_p = 100$ mW is a 93% of spontaneous Stokes radiation.

The power of Raman gain component already exceeded the SRS power at $P_p = 300$ mW. We can divide the measured value of total noise power density P_{Nt} into two parts: (i) incoherent noise with power density P_{Ns} (direct line in Figure 4) and (ii) "pure" noise amplification $P_{Nt} - P_{Ns}$, which corresponds to the area between the solid curve and the direct line in Figure 4.

We performed the separation procedure of these contributions using the model function

$$P_{Nt}(x) = axe^{kx} + bx, \tag{8}$$

which is based on (6) assuming the total noise power P_{Nt} as function of variable $x = P_p$. The slope of direct line in Figure 4 is the sum of parameters $(a + b)$. It is obviously at $k = 0$ in (8). In accordance with (6) the parameter $k = g_N L_{\text{eff}}$, where $L_{\text{eff}} = 16.77$ km for SMF at $\lambda_p = 1465$ nm.

We apply the standard procedure to find the *nonlinear fit*. It takes a model function of form (8) and then searches for values of a, b, and k parameters that yield the best fit (solid curve) to our experimental data that are shown by the black circles in Figure 4. We have obtained the set of a, b, and k parameters for the maximum noise wavelength $\lambda_s = 1568$ nm: $a = 10.94 \cdot 10^{-9}$ nm^{-1}, $b = 13.66 \cdot 10^{-9}$ nm^{-1}, and $k = 4.453$ W^{-1}. Hence, the noise Raman gain coefficient is equal to $g_{N\max} = 0.266$ W^{-1}·km^{-1} using the value of $L_{\text{eff}} = 16.77$ km.

We have made a similar analysis of the noise optical spectra for other pumping sources from a full wavelength set 1425 nm, 1435 nm, 1455 nm, and 1465 nm. The average value of $g_{N\max}$ for all λ_p neglecting the weak dependence g_N on Stokes wavelength λ_s, the dispersion of the effective area A_{eff}^{ps}, and refractive index n_p (see (3)) is obtained as

$$g_{N\max} = (0.23 \pm 0.03)\ \text{W}^{-1} \cdot \text{km}^{-1}, \tag{9}$$

which remains a constant at the accuracy of 13% for the Stokes shifts of gain maxima from 1520 nm to 1570 nm. Since $g_{R\max} = 0.38$ W^{-1}·km^{-1} [12] then the average value of coefficient η is 0.6 according to (7) and (9).

Note the spectral width of the OSA input slit of $\Delta\lambda = 1$ nm corresponded to the frequency band $\Delta\nu \approx 4$ cm^{-1} $= 1.2 \cdot 10^{11}$ s^{-1} within the range of C + L window. Thus coefficients a and b may be used to the definition of differential cross section of spontaneous Raman scattering $d\sigma_T/d\nu$, and here the linear frequency ν is measured in GHz (10^9 s^{-1}). Finally we have obtained the absolute value of $d\sigma_T/d\nu = (a + b) = 24.6 \cdot 10^{-9}$ nm^{-1} $= 2.95 \cdot 10^{-6}$ GHz^{-1} at $\lambda_s = 1568$ nm.

Therefore, the presented analysis method of ASE may be successfully used to separate the measured value of the FRA optical noise into the linear and nonlinear parts depending on the pumping power. As a result both the absolute value of the noise gain coefficient g_N and differential cross section of spontaneous Raman scattering $d\sigma_T(\nu)/d\nu$ for relatively narrow band $\Delta\nu \approx 120$ GHz are defined. However, the more practical interest is the study of FRA optical noise for C + L windows, that is, for frequency range $\Delta\nu \sim 10$ THz with very complex profile of Raman gain coefficient.

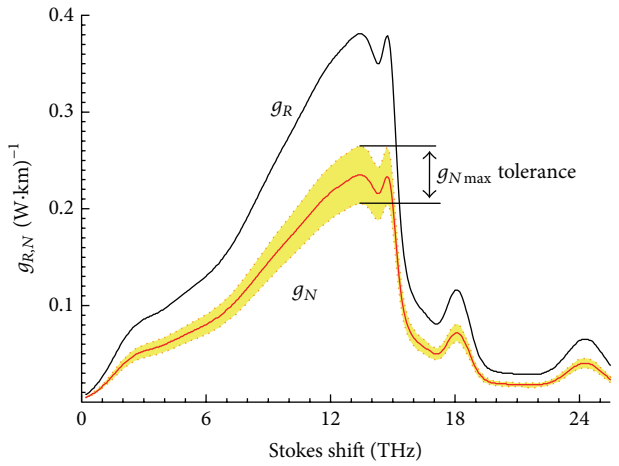

FIGURE 5: Raman gain profiles for the coherent signal wave $g_R(\nu)$ and for stochastic noise $g_N(\nu)$ in single mode silica fiber.

3.3. Raman Gain Profile for the Signal and the Noise. Raman gain profile outlined above in Section 1 is a zero Kelvin cross section. The power difference between coherent signal and incoherent noise is a result of $g_{R\max} \neq g_{N\max}$. Both profiles are presented in Figure 5 in the Stokes shifts range of 0–25.5 THz (0–850 cm^{-1}).

In general, the presented data for $g_R(\nu)$ and $g_N(\nu)$ can be used for direct calculations of the FRA noise parameters solving the coupled equations of system (5).

Note the profile of the measured spectrum $g_R(\nu)$ from [14] may be presented by an analytical form with high accuracy using the Gauss spectral decomposition [15]. It is used for both profiles plotted in Figure 5.

However, the quantitative analysis of FRA noise properties may be done in analytical form using the narrow noise band approximation.

4. Quantitative Analysis of FRA Noise Properties

The analysis of main FRA noise parameters, such as output signal to noise ratio Q_{out} and noise figure N_f can be carried out in the simplest form for a single wave of coherent signal by direct calculation using our experimental data. Both gain coefficients g_R and g_N can be considered as constants in the relatively narrow FRA bandwidth $\Delta\nu \leq 120$ GHz. The measured data of total output power P_{Nt} of Stokes noise are presented in Section 3. Let the signal power be $P_s^{\text{in}} = P_S(0)$ and total power of input noise $P_n^{\text{in}} = P_N(0)$ at the fiber input ($z = 0$). Then after the Raman amplification at the specific fiber length L the signal output power is $P_s^{\text{out}} = P_S(L)$. The total noise power is a sum $P_n^{\text{out}} = P_N(L) + P_{Nt}$, and here output own noise power P_{Nt} has been obtained. We consider the Raman gain coefficients g_R and g_N are for the amplified signal $P_S(L)$ and for the amplified input noise $P_N(L)$, respectively.

Table 1: Noise figure N_f and output B_{er} of FRA in pure silica fiber ($L = 50$ km) at two backward pump powers. It is assumed that $P_S(0) = 1$ mW and so $Q_{in}[\text{dB}] = -P_N(0)[\text{dBm}]$.

$P_N(0)$, −dBm	$P_p = 100$ mW		$P_p = 300$ mW	
	N_f, dB	B_{er}	N_f, dB	B_{er}
1	2	3	4	5
18	0.002	$4 \cdot 10^{-5}$	0.013	$4 \cdot 10^{-5}$
19	0.003	$4 \cdot 10^{-6}$	0.016	$4 \cdot 10^{-6}$
20	0.004	$3 \cdot 10^{-7}$	0.020	$3 \cdot 10^{-7}$
21	0.005	10^{-8}	0.026	10^{-8}
21.5	0.005	10^{-9}	0.029	$2 \cdot 10^{-9}$
22	0.006	$2 \cdot 10^{-10}$	0.032	$2 \cdot 10^{-10}$
22.5	0.007	10^{-11}	0.036	$2 \cdot 10^{-11}$
23	0.008	$9 \cdot 10^{-13}$	0.041	10^{-12}
23.5	0.008	$4 \cdot 10^{-14}$	0.046	$5 \cdot 10^{-14}$
24	0.009	10^{-15}	0.05	$2 \cdot 10^{-15}$
25	0.012	$3 \cdot 10^{-19}$	0.06	$5 \cdot 10^{-19}$
27	0.02	$3 \cdot 10^{-29}$	0.1	$9 \cdot 10^{-29}$
30	0.04	$4 \cdot 10^{-56}$	0.2	$4 \cdot 10^{-54}$
35	0.12	10^{-169}	0.6	$6 \cdot 10^{-152}$
40	0.36	0	1.7	0
50	2.7	0	7.6	0
	N_f 3 dB level at $Q_{in} = 50.6$ dB		N_f 3 dB level at $Q_{in} = 43.2$ dB	

Both these powers are easily calculated using (6). Particularly the signal output power is $P_s^{out} = P_S(L) = P_S(0)e^{g_R P_p L_{eff} - \alpha_S L}$. So P_s^{out} may be expressed by $P_N(0)$ as follows:

$$\begin{aligned} P_n^{out} &= P_N(0) \\ &\cdot e^{g_N P_p L_{eff} - \alpha_S L} \left\{ 1 + \frac{P_p}{P_N(0)} \left(a + be^{-g_N P_p L_{eff}} \right) e^{\alpha_S L} \right\} \\ &= P_N(0)\, e^{g_N P_p L_{eff} - \alpha_S L} \left(1 + \frac{C_N}{P_N(0)} \right). \end{aligned} \quad (10)$$

At last the expression for noise figure (1) taking the difference between g_R and g_N into account is acquired as

$$N_f = \frac{Q_{in}}{Q_{out}} = \left(1 + \frac{C_N}{P_N(0)} \right) \cdot \exp\left[(g_N - g_R) P_p L_{eff} \right]. \quad (11)$$

Note if $g_N \le g_R$ then the exponential factor is ≤1. So both FRA noise power and its N_f are maximal when $g_N = g_R$.

The physical meaning of C_N is the effective power of all optical noise reduced to FRA input. The effective power C_N contains only FRA parameters. It can be determined using the measured values in analytical form as follows:

$$C_N = P_p \left(a + be^{-g_N P_p L_{eff}} \right) e^{\alpha_S L} = P_{Nt} e^{\alpha_S L - g_N P_p L_{eff}}. \quad (12)$$

The numerical value of C_N for the known data of P_p, L, and g_N can be easily calculated either using previously determined constants a and b (see (8)) or by direct measurement data of P_{Nt} for each pump power P_p value.

If $g_N = g_R$ then (11) is maximally simplified to $N_f = [1 + C_N/P_N(0)]$. In this case the FRA "quantum limit" will be determined by equation $C_N = P_N(0)$. Then the total power of input noise $P_N(0)$ can be directly related with P_p and P_{Ns} variations using the following equation:

$$P_N(0) = P_{Ns} \exp\left(-g_R P_p L_{eff} + \alpha_S L \right), \quad (13)$$

and here it seems that $g_N = g_R$.

Direct calculations of noise figure N_f and output B_{er} of FRA in pure silica fiber ($L = 50$ km) at two backward pump powers are presented in Table 1. The typical value of the input signal power is $P_S(0) = 1$ mW (0 dBm) as commonly used in practice. Then the absolute value of the input noise power in dBm is numerically equal to the input OSNR in dB, that is, $Q_{in}[\text{dB}] = -P_N(0)[\text{dBm}]$. The B_{er} data after FRA at pumping powers of 100 mW and 300 mW are shown in columns 3 and 5 of Table 1, respectively.

Two possible cases of FRA implementation in data analysis are important:

(i) $B_{er} \le 10^{-12}$ and (ii) $N_f = 3$ dB;

(i) in this case $N_f < 0.01$ dB at $P_p = 100$ mW and $N_f \le 0.04$ dB at $P_p = 300$ mW. These N_f values may be classified as over low noise FRA amplifier with extremely low noise temperature $T_n < 1$ K;

(ii) in this case the 3 dB N_f levels are achieved at $Q_{in} = 50.6$ dB for $P_p = 100$ mW and $Q_{in} = 43.2$ dB for $P_p = 300$ mW. Under these OSNRs $B_{er} = 0$ ($B_{er} \ll 10^{-300}$); that is, amplifier also does not affect the almost complete data authenticity.

So, in both considered cases the own FRA noise does not affect the reliability of data transfer over the 50 km segment of pure silica fiber, even when $N_f > 3$ dB. On the other hand, the real noise figure at the working pump power ~300 mW can reach the values that are significantly lower than the "quantum limit" of 3 dB. In addition, one may suggest the possibility of significant extension of the fiber line length up to $L \sim 190$ km based on the data from Table 1. Here B_{er} will be $\leq 10^{-12}$ at the same power of 1 mW (0 dBm).

It is important to note that quantities of N_f are uniquely determined by measurement results of output FRA noise using (11). From another side the noise figure is dependent on both the pumping power P_p and the segment length L where the gain is realized. This nonlinear feature of distributed amplification in FRA does not allow using N_f as generalized parameter of FRA in contrast to lumped electronic devices. The N_f value does not determine B_{er} of the total data link without specifying the length L and the ratio of pumping power P_p to input noise power. In addition the unique property of nonlinear amplification in FRA is shown by the powerful gain g_R exceeding over the gain g_N of weak stochastic optical noise. It can be the result of $N_f < 1$. In this case optical signal to noise ratio can increase at the output of fiber length of 50 km. However, the output B_{er}, as we see, can be easily calculated according to direct measurements of output power of optical noise at the idle FRA despite the ambiguity of the parameter N_f.

Thus the optical noise figure in real FRA working mode is on the level lower than the earlier limit of 3 dB. This fact eliminates the above contradiction between previous theory and many present experimental works.

In summary of this section the quantitative analysis of FRA noise properties was made using the simplest model of a single signal wave in relatively narrow FRA bandwidth. But we assume the common features of noise in FRA will be valued in the more general cases due to distributed amplification and Raman gain nonlinearity.

5. Conclusions

The detailed analysis of noise properties of distributed Raman gain in the 50 km segment of single mode silica fiber is presented. Main results were obtained:

(1) The Raman gain coefficient for noise amplification in pure silica fiber is obtained as $0.23\,(\mathrm{W{\cdot}km})^{-1}$ based on our experimental data. It indicates substantial difference from the gain of coherent signal.

(2) It is shown the optical noise figure in the real FRA working mode can be widely varied. In particular, its level can be significantly lower than the quantum limit of 3 dB.

(3) The method of ultimate B_{er} determination using the direct measurements of the output power of optical noise at the idle FRA is proposed. Our method is applied to FRA noise analysis and it is free on the ambiguity of N_f parameter.

Thus our results show the improvement of noise properties in distributed FRA. It confirms our hypothesis about noise figure existence below the quantum limit.

Competing Interests

The authors declare that there is no conflict of interests regarding the publication of this paper.

References

[1] P. A. Korotkov and G. S. Felinskyi, "Forced-Raman-scattering-based amplification of light in one-mode quartz fibers," *Ukrainian Journal of Physics. Reviews*, vol. 5, no. 2, pp. 103–169, 2009.

[2] S. L. Aquea, R. Olivares, and B. D. Feris, "Flat-gain DFRA design considering pump-to-pump FWM," in *Proceedings of the International Workshop on Fiber Optics in Access Network (FOAN '12)*, pp. 583–586, St. Petersburg, Russia, October 2012.

[3] M. N. Islam, Ed., *Raman Amplifiers for Telecommunications 2: Sub-Systems and Systems*, Springer, New York, NY, USA, 2004.

[4] G. P. Agrawal, *Fiber-Optic Communication Systems*, John Wiley & Sons, New York, NY, USA, 3rd edition, 2002.

[5] Y. Yamamoto and K. Inoue, "Noise in amplifiers," *Journal of Lightwave Technology*, vol. 21, no. 11, pp. 2895–2915, 2003.

[6] H. A. Haus, "Noise figure definition valid from RF to optical frequencies," *IEEE Journal on Selected Topics in Quantum Electronics*, vol. 6, no. 2, pp. 240–247, 2000.

[7] C. H. Henry and R. F. Kazarinov, "Quantum noise in photonics," *Reviews of Modern Physics*, vol. 68, no. 3, pp. 801–853, 1996.

[8] P. B. Hansen, L. Eskildsen, S. G. Grubb et al., "Capacity upgrades of transmission systems by Raman amplification," *IEEE Photonics Technology Letters*, vol. 9, no. 2, pp. 262–264, 1997.

[9] C. Headley and G. P. Agrawal, *Raman Amplification in Fiber Optical Communication Systems*, Elsevier Academic Press, San Diego, Calif, USA, 2005.

[10] R. H. Stolen, E. P. Ippen, and A. R. Tynes, "Raman oscillation in glass optical waveguide," *Applied Physics Letters*, vol. 20, no. 2, pp. 62–64, 1972.

[11] K. Rottwitt, J. Bromage, A. J. Stentz, L. Leng, M. E. Lines, and H. Smith, "Scaling of the Raman gain coefficient: applications to germanosilicate fibers," *Journal of Lightwave Technology*, vol. 21, no. 7, pp. 1652–1662, 2003.

[12] J. Bromage, "Raman amplification for fiber communications systems," *Journal of Lightwave Technology*, vol. 22, no. 1, pp. 79–93, 2004.

[13] M. Y. Dyriv, G. S. Felinskyi, and P. A. Korotkov, "Fiber attenuation irregularities and simulation of Raman amplification band," in *Proceedings of the 12th International Conference on Laser and Fiber-Optical Networks Modeling (LFNM '13)*, pp. 44–46, Sudak, Ukraine, September 2013.

[14] F. Emami and A. H. Jafari, "Theoretical optimum designation of distributed Raman amplifiers in different media," *WSEAS Transactions on Communications*, vol. 8, no. 2, pp. 249–258, 2009.

[15] M. Dyriv, P. Korotkov, and G. Felinskyi, "Raman gain profile simulation in single-mode fibers using spectral decomposition," *Bulettin of Taras Shevchenko National University of Kyiv, Radiophysics and Electronics*, vol. 18, pp. 15–18, 2012.